



## **THEORETICAL ANALYSIS AND COMPUTER SIMULATION OF THE PARTICLE GRADIENT DISTRIBUTION IN A CENTRIFUGALLY CAST FUNCTIONALLY GRADIENT MATERIAL**

**Prem E. J. Babu, T.P.D. Rajan, S. Savithri, U.T.S. Pillai and B.C. Pai**  
*Regional Research Laboratory, Trivandrum, India.*

### **ABSTRACT**

Two-dimensional dynamics simulations are carried out using a developed analytical theory, for engineering a desired composition gradient, in centrifugally cast metal-ceramic functionally gradient materials (FGM). For this purpose, the motion of ceramic particles in a viscous molten metal under centrifugal force is first modeled and the effects of solidification were incorporated. The process of gradient composition formation under the centrifugal force is then simulated by considering the movement of each particle suspended in the viscous metal. The concoction of aluminium and silicon carbide (SiC) particles are chosen to make the FGM rings by the centrifugal method. The simulations are validated with the experimental results and hence the applicability of the proposed simulation technique to engineer a desired composition gradient in FGM is discussed.

**Keywords:** gradient materials, centrifugal casting, viscous flow, computer simulation

### **1. INTRODUCTION**

Functionally gradient materials (FGMs) are epitomized by continuous and smooth variations in compositions and/or microstructure, so as to meet the functional performance requirements that vary with location within a part. Among various FGMs, metal-ceramic FGMs, also called metal matrix composite FGMs are of great practical interest. These FGMs feature gradual compositional variations from metal concentrated region at one surface to ceramic concentrated region at the other, leading to controlled gradation of physical, mechanical and/or chemical properties across the thickness accompanied by minimized stress concentration at the interface of dissimilar materials. Therefore, such FGMs are rapidly finding applications in aggressive environments with steep temperature gradients such as rocket nozzles, thermal barrier coatings, turbine components etc, and in some typical automobile components.

However, at present there is no reliable and inexpensive way of fabricating FGMs that allows mass production of large components. Current methods of fabrication include solidification processing, chemical vapor deposition, spray atomization and co-deposition, and powder metallurgy techniques<sup>1, 2</sup>. Of these, perhaps the most economical and attractive processing route is gravity or centrifugal casting. This process involves the addition of a reinforcing particle phase to a molten metal matrix, mixing them uniformly followed by segregation of particles and liquid in a gravitational or centrifugal field to get a composition gradient due to a difference in density between the phases and finally preserving the graded structure by solidification.

Among the two, the centrifugal separation finds further attraction owing to the fact that a controlled gradient can be obtained by controlling the processing parameters. Metal-ceramic

FGMs had been successfully synthesized by this method. However, the technology still remains in the experimental trial out stage, mainly due to the lack in accurate controlling and understanding the distribution of particles. The critical processing parameters that decide the final gradient microstructure includes the crucible furnace temperature, mold heating furnace temperature, thermal gradient across the mold, pouring rate, velocity of mold rotation, solidification rate etc. However, the determination of temperature distribution during centrifugal casting by experimental techniques is very difficult, as the mold rotates at a very high speed during solidification. Moreover, estimation of the solidification through heat and mass transfer analysis under realistic conditions during centrifugal casting is an intricate problem to work out<sup>3</sup> and hence earlier works done on centrifugal casting of FGMs does not take into account of the solidification effects, while modeling the particle distribution pattern with respect to processing parameters<sup>4-6</sup>.

Hence, an effort has been made to incorporate the effect of the solidification front together with the other effects to predict the distribution pattern obtained during centrifugal casting. For modeling the system, the molten metal is regarded as a viscous liquid and the motion of ceramic particles in the viscous liquid under a centrifugal force is concerned. Considering the movement of each particle that is suspended in the viscous liquid under the centrifugal force and the other forces, the microstructure or composition gradient formation is simulated. Mixtures consisting of aluminium matrix and SiC particles are chosen for the experiments and rings having various graded compositions are manufactured by the centrifugal casting setup fabricated in the laboratory. The validity of the method for engineering the desired composition gradient in FGMs is discussed by comparing the experimentally obtained gradient with those acquired from computer simulations.

## 2.0 MODELING AND SIMULATION

### 2.1 Governing Equations

During casting of metal-ceramic FGM rings, the system of ceramic particles in molten metal behaves as a suspension of hard particles in a viscous liquid. Due to centrifugal action, the hard particles will be pushed towards the outer or inner periphery due to the density difference between the particles and the liquid melt (If the particle is having a higher density than the fluid, the particles will move outward and vice versa). The viscous drag force exerted by the fluid will oppose the motion of particles due to the centrifugal force. In addition, when such a liquid containing a dispersion of particles is solidified, the solidification front will exert a repulsive force on the particle and push them along with it. Moreover, the particles that are suspended in molten metal will also suffer a gravity force. However, compared to the centrifugal force, gravity forces are very and hence the vertical movement of the particle can be ignored.

A typical FGM microstructure having a graded microstructure is shown in Fig. 1. Fig. 2(a) illustrates the force fields, where particles in a liquid will be acted on by centrifugal, gravity and drag forces and the interaction between the particle and the interface of the particle movement (solidification front) under the influence of centrifugal forces are shown in Fig. 2(b).

#### 2.1.1 The Centrifugal Force

During centrifugal casting, particle segregation occurs owing to difference in densities between the molten metal and the particles. Then a particle which is suspended in a molten metal is submitted to a centrifugal acceleration of  $\Upsilon = \omega^2 r$ , where  $r$  is the radial position of the particle. Assuming spherical particles, the total centrifugal force is given by

$$F_c = m\omega^2 r = \frac{4}{3} \pi R_p^3 (\rho_p - \rho_l) \omega^2 r \quad (1)$$

### 2.1.2 Repulsive force by the solidification front

The repulsive force acting across the melt-filled gap between the solidification front and the particle is modeled as arising due to van der Waals interaction forces. Shangguan and coworkers<sup>7</sup> derived a simple form of equation for this repulsive force, by assuming this force as a van der Waals force between a spherical particle and a plane wall. The van der Waals force is the force due to the interfacial energy, which occurs as the interface or solidification front approaches the particle closely enough, i.e., at a distance of the order of atomic spacing. This repulsive force is therefore called as a molecular force and the expression for this force is given by

$$F_s = 2\pi R_p \Delta\gamma \quad (2)$$

This was calculated as the energy required moving the particle over a unit distance into the solid. The interface energy term is defined as

$$\Delta\gamma = \Delta\gamma_0 \left( \frac{a_0}{a_0 + d} \right)^2 \quad (3)$$

where,  $a_0$  is the atomic distance (molecular diameter of the matrix material) and  $d$  is the gap between the tip of the solidification front and the particle and the repulsive force between a solid spherical particle and a solid-liquid interface results from the difference in surface tension  $\Delta\gamma_0$  as

$$\Delta\gamma_0 = (\gamma_{PS} - \gamma_{PL} - \gamma_{SL}) \quad (4)$$

where,  $\gamma_{PS}$ ,  $\gamma_{PL}$  and  $\gamma_{SL}$  are the solid-particle, particle-liquid and solid-liquid interfacial energies.

### 2.1.3 The Drag Force

The movement of the particle due to the above-discussed repulsive force necessitates a flow of liquid into the gap, which exerts a drag force on the particle. In the case of flow over a sphere, both friction drag and pressure drag (form drag) contribute to total drag. Stokes<sup>8</sup> reported that for a symmetric flow field with small velocities ( $Re < 0.1$ ), the dominant force on the sphere is viscous and the inertial term in the momentum equation can thus be neglected. The expression given by Stokes<sup>8</sup> is

$$F_D = 6\pi R_p \mu V_p = 6\pi R_p \mu \frac{dr}{dt} \quad (5)$$

where,  $\mu$  is the kinematic viscosity of the fluid material.

### 2.1.4 Particle Movement

The particle in the molten metal under the centrifugal force suffer all the above three forces, and hence the motion of particles are controlled by these forces. However, during solidification, pushing/engulfment of particles occur at the solid-liquid interface. Therefore, before making the dynamic force balance, a check has been conducted to find out, whether pushing or engulfment is happening in the FGM.

#### 2.1.4.1 Condition for pushing/engulfment

The three forces on the particle play different roles in the pushing/engulfment transition. For inward growth of the solidification front,

- $F_C$  assist to pushing if  $\Delta\rho > 0$
- $F_S$  assist to pushing if  $\Delta\gamma_0 > 0$  and assist to engulfment if  $\Delta\gamma_0 < 0$ , and
- $F_D$  always assists to engulfment

The parameters for the present Al-SiC system are given in Appendix 1. (From the calculations based on the constants and using the formulas discussed under section 2.2.2, it has been observed that  $\Delta\rho > 0$  and  $\Delta\gamma_0 > 0$ .)

#### 2.1.4.2 Dynamic equation

The net force required to accelerate the particle is balanced by the drag force, the force exerted by the solidification front and the centrifugal force. Since  $F_C$  and  $F_S$  assists to pushing and  $F_D$  assist to engulfment, the dynamic equation to describe the particle movement can be written as a second-order differential equation based on Newton's second law as

$$\frac{4}{3}\pi R_p^3 \rho_p \frac{d^2 r}{dt^2} = F_C + F_S - F_D \quad (6)$$

The complete solution to the above problem is obtained after a lengthy derivation. The final solution takes the form

$$r = C_1 e^{m_1 t} + C_2 e^{m_2 t} + C_3 \quad (7)$$

where,  $C_1$ ,  $C_2$ ,  $C_3$ ,  $m_1$  and  $m_2$  are sub-equations obtained by solving Eqn. (6), and 'r' represents the position of the particle at time 't'. The sub-equations in Eqn. (7) involves constants like density terms, initial position of the particles,  $\Delta\gamma$ ,  $a_0$  etc, and variables like viscosity of the melt having particles, size and shape of the particles, volume percent of the phases, speed of rotation of the mold, etc.

### 2.2 Computer Simulations

The various parameters that are varied to obtain a desired gradient in the FGMs involve the volume fraction of particles in the melt, applied centrifugal force, force exerted by the solidification front, holding time and the ring thickness.

#### 2.2.1 Viscosity of the melt

It is known that the viscosity of the melt increases according to the increase in number of particles in the suspension. The viscosity of a melt containing particles is given by<sup>9</sup>

$$\mu = \mu_0 (1 + 2.5V_p + 10.05V_p^2) \quad (8)$$

where,  $\mu_0$  is the viscosity of the molten metal without particles and  $V_p$  is the particle volume fraction in the melt.

#### 2.2.2 Thermodynamic calculations for the Al-SiC system

The interface tension between the SiC particle and the liquid Al,  $\gamma_{PL}$  is calculated with the Young's equation:

$$\sigma_{PL} = \sigma_{PV} - \cos \Theta \sigma_{LV} \quad (9)$$

where,  $\Theta$  is the contact angle of Al on the SiC particle.

The interfacial tension can also be determined by means of Neumann's equation of state approach<sup>10</sup>, using the relation:

$$\sigma_{PL} = \frac{(\sigma_{PV}^{1/2} - \sigma_{LV}^{1/2})^2}{1 - k(\sigma_{PV}\sigma_{LV})^{1/2}} \quad (10)$$

The substitution of the value for  $\sigma_{PL}$  from Eqn. (9) in Eqn. (10) yields the value of the constant 'k'. Now, the surface tension between solid and liquid Al,  $\sigma_{SL}$ , as well as that between SiC and Al,  $\sigma_{PS}$ , can be calculated in a similar fashion of Eqn. (10). Once all the surface energies are established, the value for  $\Delta\gamma_0$  can be calculated using Eqn. (4).

### 3.0 RESULTS AND DISCUSSIONS

#### 3.1 Particle distribution in experiments

FGM rings of 16mm thickness having SiC particle gradation in a 2124-Aluminium base matrix are manufactured using the centrifugal casting setup fabricated in the laboratory, for the validation of the computer simulation. The SiC particle size used in the FGM is 23 $\mu$ m and the speed of rotation of the mold was set at 1140 rpm. The volume fraction of SiC is 0.15 in all the experiments and the same is used in the simulations also. Fig. 3 shows some of the castings made out of the centrifugal casting process using the above-said parameters.

It can be observed from the figure that the obtained castings from the centrifugal casting are having less defects and good surface finish. To examine the gradient pattern obtained in the castings, micrographs are taken across the section at various locations and are shown in Fig. 4. The microstructures are given from the outer periphery towards the inner periphery at different positions (in mm). It is clear from the micrographs that the particle concentration gradually decreases from the outer end towards the inner end of the casting.

The important aspects noted from the micrographs is that very few particles are observed above 8mm from the outer end of the casting and a particle concentration more than 50% is observed at the outer end of the casting. This shows a clear segregation effect during centrifugal casting.

#### 3.2 Particle distribution in simulations

In order to validate the proposed theory, computer simulation of real-time Al-SiC system was performed using a code developed in Visual C++. The system taken for the simulation is the same as used in the experiments (SiC particle reinforced 2124-Aluminium FGM). The solidification rate of this system was observed as 400  $\mu$ m/sec, and hence the time required for the complete solidification of the 16 mm casting was calculated to be 40 seconds. The simulation results were taken at 5 sec, 10 sec, 20 sec and 40 sec and are shown in Figs. 5 (a) – 5(d). The gradient formation process was noticed at small intervals albeit only four set of plots were shown here for comparisons. For getting a clear visualization, the particles getting the same coordinate positions were altered along the y-axis, maintaining the same particle volume fraction at that specified locations. Better agreement was observed with the simulation and the trend observed in the experiments.

### 3.3 Engineering a desired composition gradient

The composition gradient formation process mainly depends on the density difference between the phases, speed of rotation of the mold, particle size and shape, viscosity of the melt, particle volume fraction, thickness of the cast ring and the solidification time. It is apparent that density,  $\Delta\gamma$ ,  $a_0$  and viscosity are material constants and particle volume fraction, thickness etc. are constants of the end-product. Moreover, the solidification time depends mainly on the convection cooling due to the speed of rotation of the mold and the initial position of the particles in the melt depends on the type of stirring and the baffles used. Hence, a possible and easily variable parameter is the particle shape and size. Therefore, the composition gradient formation process in FGM can be easily controlled by using different mesh size particles.

For determining the mesh sizes according to the designer's specific needs, the present theory and the simulation find extensive use. Moreover, the proposed simulation technique is very user-friendly, so that modifications can be done at any stage of its processing.

### 3.4 Significance and scope of the present work

The unique aspect of the proposed analytical framework lies in the fact that all the forces acting on the particle during centrifugal separation process has been considered. Moreover, solution of a second order theory in the simulation of gradient formation process is the first of its kind and hence a refined solution is possible with the present theory. The previous works dealt with solving a first order theory in this regard<sup>3-6</sup>. Moreover, the code employed for performing the numerical simulation is formulated in a simple manner, so that the parameters in the code can be easily varied, and thus can be explicitly employed to any type of FGM systems. The variables such as particle volume fraction and particle size can be easily incorporated by changing the values for the corresponding variables. In a similar fashion, the effect of various particle shapes can be simulated by altering the equations for the viscous drag and the particle volume. Thus the present work will be extremely useful to have a clear-cut understanding concerning the process of gradient formation and helps in engineering the gradient in FGMs as per the end-user needs.

## 4.0 SUMMARY/CONCLUSIONS

In this study, a unique theory has been developed to simulate the process of gradient formation during centrifugal casting of FGMs. The theory embodies the solidification effects in concert with the other major forces (centrifugal force and the viscous drag force). For the purpose, the motion of ceramic particles in a viscous molten metal under centrifugal force is considered and the process of gradient formation under the centrifugal force is then simulated by considering the movement of each particle that is suspended in the viscous metal. The gradient pattern of SiC particles in aluminium matrix were analyzed at various time steps, using the simulation and are compared with the results obtained from centrifugal casting experiments to validate the efficiency of the theory. Moreover, the applicability of the proposed theory in engineering the process of gradient formation in FGMs is discussed.

## 5.0 ACKNOWLEDGEMENTS

The financial support from The Council of Scientific and Industrial Research (CSIR), Govt. of India and The Department of Science and Technology (DST), Govt. of India for the first and second authors respectively are deeply acknowledged. The authors are grateful to Mr. K.R. Hafiz and Mr. K.S. Shibu for rendering their extensive support during the experiments. The helpful discussions with Mr. K.R. Ravi, Mr. A. Srinivasan, Ms. K.K. Usha, Ms. V. Subashini and Mr. G. Sudarshan Rao are also greatly appreciated.

## 6.0 REFERENCES

1. Mortensen A. and Suresh S., *Int. Mater. Rev.*, 40 (1995), 239.
2. Ho S. and Lavernia E.J., *Metall. Mater. Trans. A*, 27A (1996), 3241.
3. Kang C.G. and Rohatgi P.K., *Metall. Mater. Trans. B*, 27B (1996), 277.
4. Watanabe Y, Kawamoto A, and Matsuda K, *Compos. Sci. Tech.* 62 (2002) 881.
5. Poolthong N, Qui P, and Nomura H, *Sci. Tech. Adv. Engng. Mtls.* 4 (2003) 481.
6. Watanabe Y, Yamanaka N, and Fukui Y, *Composites A*, 29A (1998), 595.
7. Shangguan D, Ahuja S, and Stefanescu D.M, *Metall. Trans.A*, 23A (1992) 669.
8. Stokes G.G, *Trans. Cambridge Phil. Soc*, 9, II (1851) 8.
9. Stefanescu D.M. and Dindaw B.K., In *Metals Handbook*, Vol. 15, Metals Park, OH, ASM International (1988) p.142.
10. Omenyi S.N and Neumann A.W, *J. Appl. Phys.* 47 (1976) 3956.

### Appendix: I

Numerical values used <sup>7</sup>

Viscosity of molten Al =  $2 \times 10^{-3}$  Pa.s

Contact angle of Al on SiC at 950 °C = 120 deg

Acceleration due to gravity  $g = 9.81 \text{ m/s}^2$

Interface energies:

$$\gamma_{PV} \text{ for SiC at } 1430^\circ\text{C} = 1.844 \text{ J/m}^2$$

$$\gamma_{LV} \text{ for Al at } 950^\circ\text{C} = 0.84 \text{ J/m}^2$$

$$\gamma_{SV} \text{ for Al at melting point} = 0.98 \text{ J/m}^2$$

Densities:

$$\rho_{\text{AL}} = 2.36 \times 10^3 \text{ kg/m}^3$$

$$\rho_{\text{SiC}} = 3.22 \times 10^3 \text{ kg/m}^3$$

Atomic distance in Al =  $3 \times 10^{-8} \text{ m}$

## FIGURES

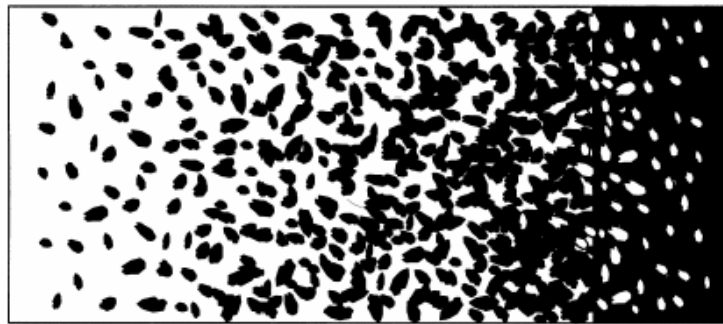


Fig. 1 Typical FGM representation having a gradient microstructure (black patches show the second phase selectively reinforced in the white matrix)

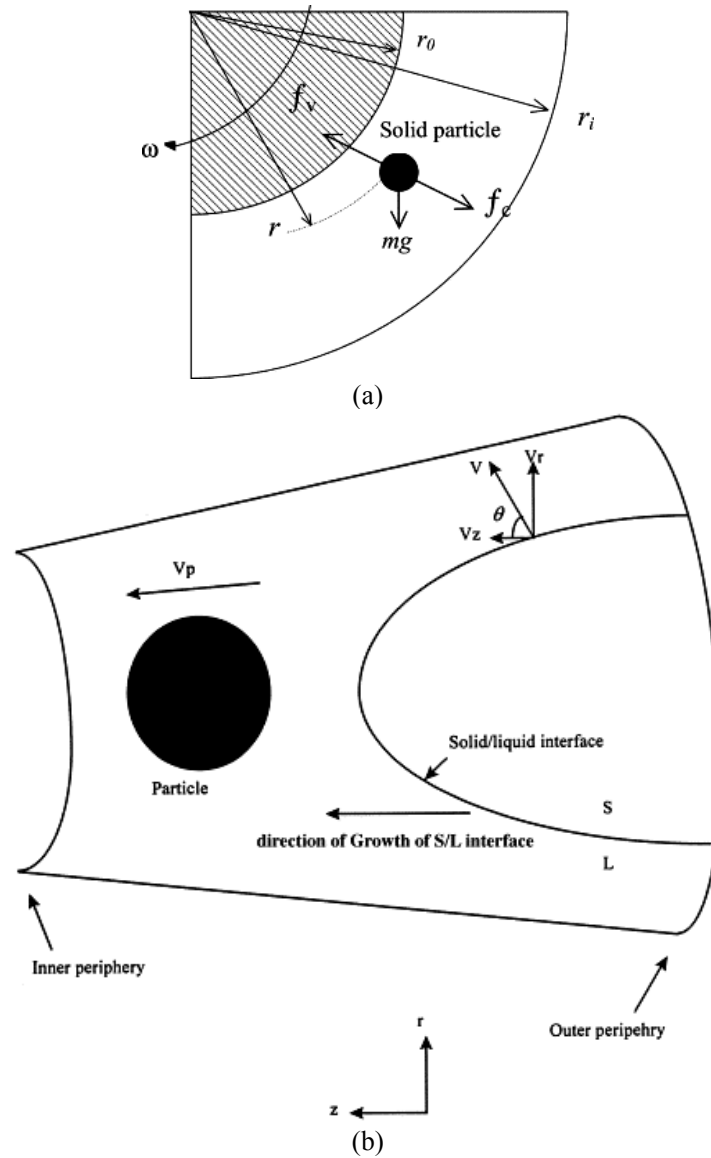


Fig. 2 (a) Force fields on the particle suspended in the viscous melt (b) The schematic depiction showing the interaction between the particle and the interface of the particle movement under the influence of centrifugal forces



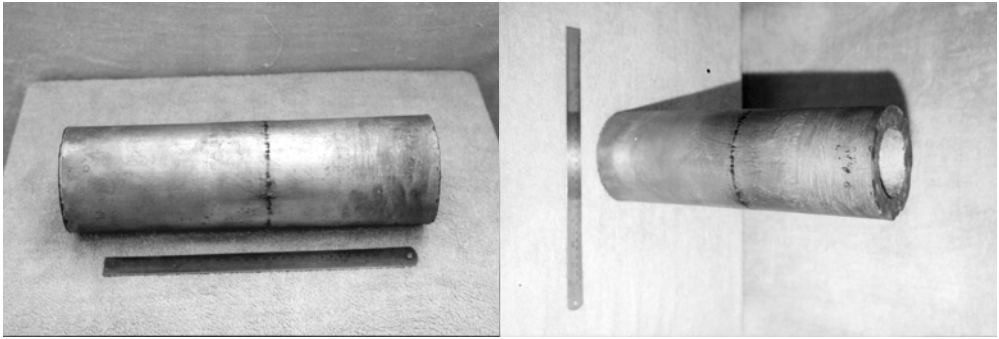
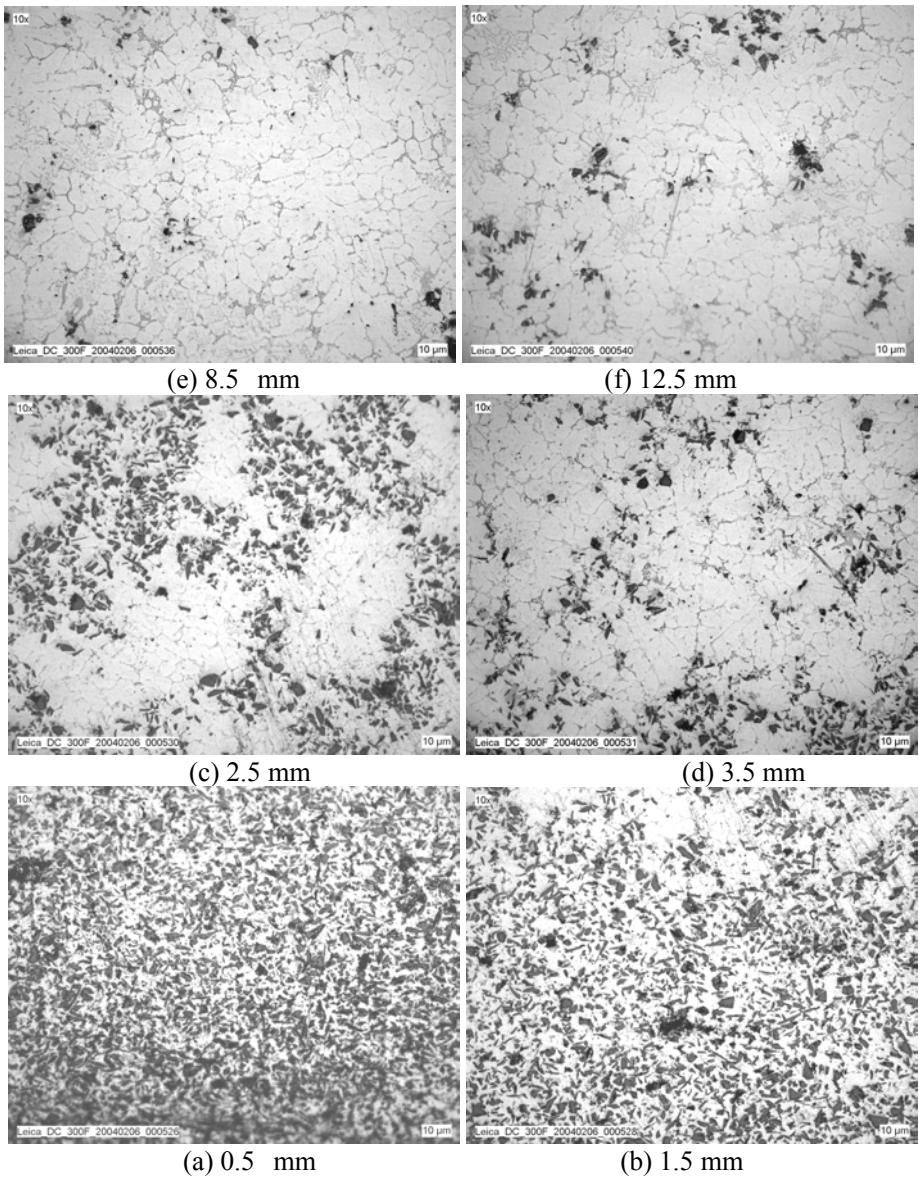


Fig. 3 Cylinder liner castings made out of the centrifugal casting process



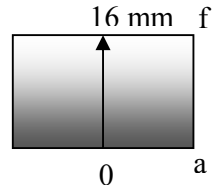


Fig. 4 Microstructures of 2124Al-SiC FGM hollow cylinder fabricated by horizontal centrifugal casting (taken at various thickness)

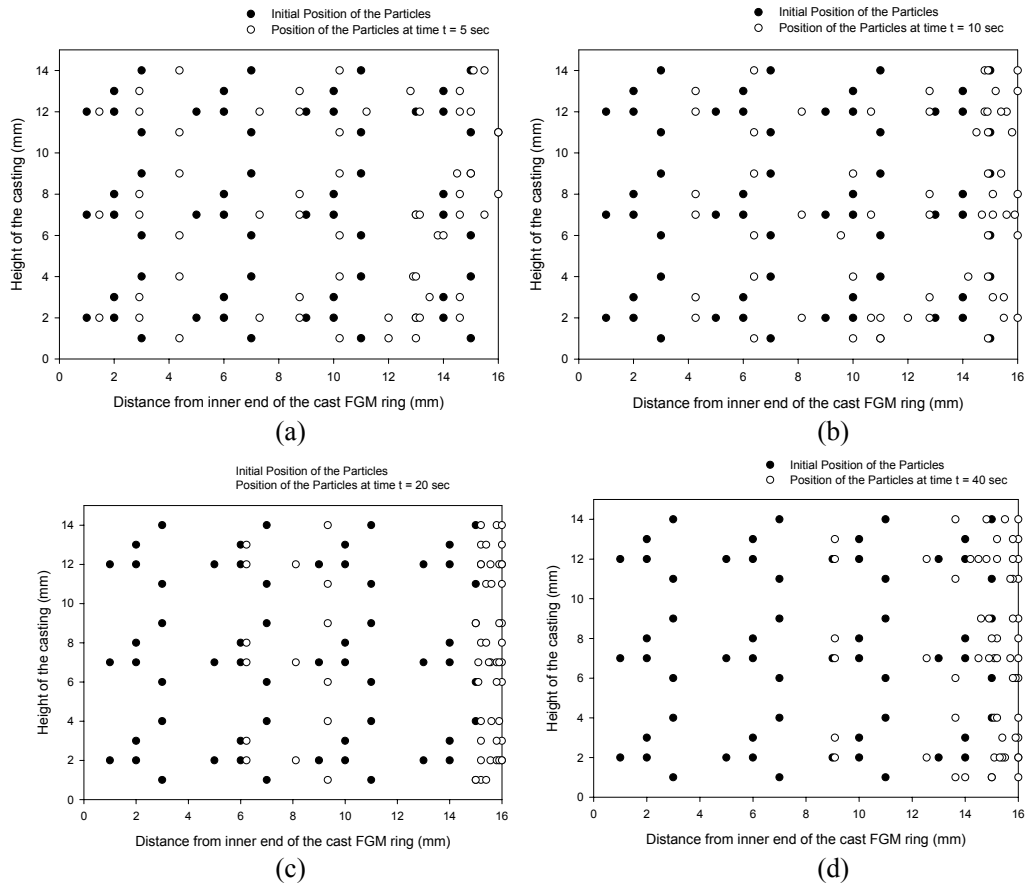


Fig. 5 Particle distribution patterns obtained from the simulations after  
(a) 5 sec (b) 10 sec (c) 20 sec (d) 40 sec